JOURNAL OF MATERIALS SCIENCE 16 (1981) 2846–2854

# Fatigue analysis of brittle materials using indentation flaws

## Part 1 *General theory*

B. R. LAWN, D. B. MARSHALL*, G. R. ANSTIS†, T. P. DABBS
*Department of Applied Physics, School of Physics, University of New South Wales, Kensington, NSW 2033, Australia*

A two-part study has been made of the fatigue characteristics of brittle solids using controlled indentation flaws. In this part a general theory is developed, with explicit consideration being given to the role played by residual contact stresses in the fracture mechanics to failure. The distinctive feature of the formulation is a stress intensity factor for well-defined indentation cracks, suitably modified to incorporate the residual component. Taken in conjunction with a standard power-law crack velocity function, this leads to a differential equation for the dynamic fatigue response of a given material/environment system. Reduced variables are then introduced to facilitate generation of "universal" fatigue curves, determined uniquely by the crack velocity exponent, $n$. A scheme for using these curves to evaluate basic fracture parameters from strength data is outlined. In this way the foundation is laid for lifetime predictions of prospective brittle components, as well as for reconstruction of the crack velocity function. One of the major advantages of the analysis is the manner in which the residual stress parameters are accommodated in the normalized fracture mechanics equations: whereas it is understood that *all* strength data are to be taken from test pieces in their as-indented state, so making it unnecessary to have to resort to inconvenient stress-removal procedures between the contact and failure stages of testing, *a priori* knowledge of the residual stress level is not required. The method is proposed as an economical route to materials evaluation and offers physical insight into the behaviour of natural flaws.

### 1. Introduction

The tendency for brittle glasses and ceramics to exhibit limited lifetimes under conditions of sustained loading is a direct manifestation of chemically-assisted flaw growth [1]. A proper study of so-called "fatigue" behaviour is accordingly an essential element of structural design with brittle components. Central to most modern-day analyses of fatigue is the fracture mechanics concept of a well-behaved "Griffith flaw" which extends from its initial size to a failure configuration in accordance with some specifiable crack velocity function. Unfortunately, *a priori* knowledge of the flaw parameters needed for long-term lifetime prediction is generally unavailable, so it becomes necessary to characterize the flaw population in terms of data from control strength tests. This line of attack suffers from two major drawbacks: first, because of a common tendency to a large scatter in flaw severity from specimen to specimen with as-received surfaces, an inordinately large number of tests has to be carried out in order to obtain statistically meaningful data for materials evaluation; second, because identification of the specific flaw ultimately responsible for failure is usually possible by test-piece examination only after the event, the

*Present address: Materials and Molecular Research Division, Lawrence Berkeley Laboratory, University of California, Berkeley, California 94720, USA.
†Present address: Department of Metallurgy and Science of Materials, University of Oxford, Oxford, UK.

 0022–2461/81/102846–09$02.90/0 

crack evolution can not be followed directly. The trend in engineering design has been for data manipulation to supplant physical insight as the underlying basis of fatigue analysis.

One way of avoiding the problems of variability in strength testing is to introduce dominant flaws by controlled indentation [2–4]. Recent studies in these laboratories along such lines have been made on the dynamic [5] (constant stress rate) and static [6] (constant stress) fatigue properties of soda-lime glass in the presence of water. In these studies the high degree of data reproducibility asssociated with the "indentation/strength" approach proved to be particularly useful for the determination of accurate kinetic constants in the crack velocity equation. More importantly, from detailed observations of the crack response throughout its history prior to test-piece failure [4, 5], it was unequivocally demonstrated that flaws could behave in a manner quite unlike that of the classical Griffith sense, with important implications in lifetime prediction [6]. Specifically, cracks formed in an elastic–plastic contact field using a sharp indenter are subject to a residual driving force [3, 7] and this residual force has a profound influence on the fracture mechanics to failure. Such effects would be felt in any naturally occurring flaw whose nucleation forces persisted in whole or in part in the material [8].

In this investigation, presented in two parts, we illustrate how the indentation/strength procedure can be used to determine the fatigue characteristics of brittle materials. Part 1 outlines the general theory, and Part 2 presents a case study on a "typical ceramic". Whereas in our previous fatigue studies on soda-lime glass [5, 6] emphasis was placed on establishing the validity of the fracture mechanics formulation, especially with regard to the residual stress component, in this work we concern ourselves more with the practical issue of materials evaluation. In the interest of experimental simplicity, the fatigue data are assumed to be taken exclusively from test-pieces in the "as-indented" state: the analytical complexity that attends the consequent need to deal with the residual stresses is considered more than offset by not having to remove these stresses by physical means (e.g. by annealing or surface grinding [9, 10], processes which could significantly alter the very nature of the flaws, or even of the material itself). Moreover, this additional complexity can be minimized by judicious choice of reduced variables, so that the need to specify an appropriate residual-stress parameter is avoided. Adoption of a Vickers hardness indenter for introducing the starting flaws, and of constant stress rates in the breaking routine, allows for convenient standardization of the procedure without seriously affecting the generality of the analysis.

## 2. Theory of dynamic fatigue for indentation flaws

### 2.1. Basic fracture mechanics formulation

In this subsection we summarize the basic features of the fracture mechanics formulation [5, 6]. A schematic diagram of the model indentation flaw system is given in Fig. 1. It is assumed that the specimen surface is free of all stresses prior to indentation. The indentation event itself produces a well-defined crack system, whose characteristic size $c$ depends on the peak contact load $P$. Subsequent application of a tensile stress $\sigma_a$ causes the

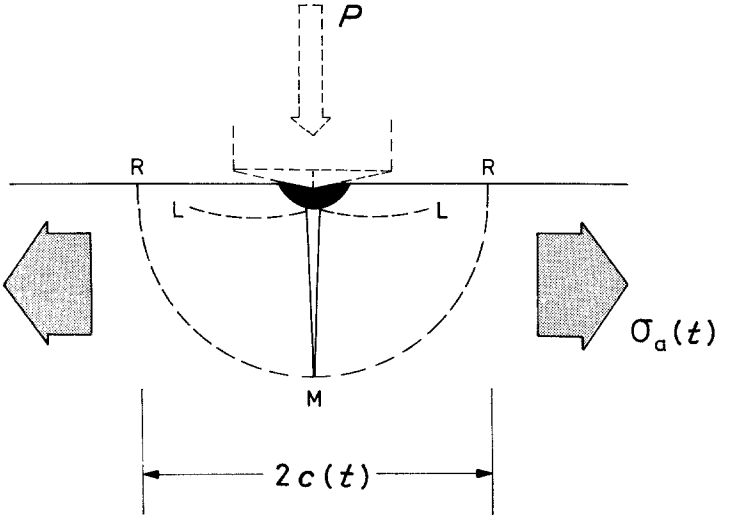


*Figure 1* Schematic diagram of Vickers-produced radial/median (RM) crack system, formed at peak indentation load $P$ and subject to expansion in characteristic dimension $c$ under subsequent application of tensile stress $\sigma_a$. Also shown is lateral (L) crack system and central deformation zone (shaded).

crack system to grow toward an instability configuration. The crack which controls the strength is of the "radial/median" type [7]. For the Vickers indentation geometry depicted in Fig. 1 there are two such cracks, orthogonal to each other and semicircular about the origin of contact; both may expand under the action of the applied stress (depending on whether this stress is uniaxial or biaxial), but we focus our attention on the one ultimately responsible for failure. A second system of cracks, of the "lateral" type [11, 12], remains passive during strength testing. All of the cracks originate from the central deformation zone, which is also the source of the residual driving force. The stress intensity factor for the dominant radial/median crack may then be written

$$K = \frac{\chi_r P}{c^{3/2}} + \sigma_a(\pi\Omega c)^{1/2} \qquad (c \geqslant c_0), \quad (1)$$

i.e. as the sum of residual-contact and applied-stress components: $\chi_r$ is a parameter of the elastic–plastic indentation field, determined for any given material by the ratio of hardness to Young's modulus [7]; $\Omega$ is a crack geometry parameter, equal to $4/\pi^2$ for an ideal centrally-loaded penny crack [13] but here modified by the presence of crack neighbours, deformation zone and specimen free surface. The crack length $c_0$ pertains to the immediate post-indentation configuration, at which point the equilibrium condition $K = K_c$, where $K_c$ is the toughness, is satisifed [7]. Putting $\sigma_a = 0$ in Equation 1 then gives $c_0 = (\chi_r P/K_c)^{2/3}$ as an initial condition for the ensuing strength test. In reality, it is not easy to avoid exposing the indented surface to a reactive environment (especially moisture, in the case of many ceramics), so the crack may extend subcritically to some non-equilibrium size $c_0'$ prior to application of the tensile stress [3–6]. Also, the parameters $\chi_r$ and $\Omega$ may be subject to departures from constancy during the various stages of crack evolution [5, 14], suggesting that care needs to be exercised in specifying the terms in Equation 1.

Before considering fatigue effects in any detail it is useful to treat the special case where the strength test is carried out in an inert environment. The resulting "inert strength" then serves as a convenient baseline for data reduction. Inserting the equilibrium requirement $K = K_c$ into Equation 1 and solving for $\sigma_a$ gives

$$\sigma_a = \left[\frac{K_c}{(\pi\Omega c)^{1/2}}\right]\left[1 - \frac{\chi_r P}{K_c c^{3/2}}\right]. \quad (2)$$

The function $\sigma_a(c)$ passes through a maximum, $\sigma_m$, at

$$\sigma_m = \frac{3K_c}{4(\pi\Omega c_m)^{1/2}} \quad (3a)$$

with

$$c_m = \left(\frac{4\chi_r P}{K_c}\right)^{2/3}. \quad (3b)$$

In the crack-size range $c_0 \leqslant c < c_m$ the equilibrium remains stable, so the crack undergoes a stage of precursor growth as the stress is raised; at $c = c_m$ the configuration becomes unstable and failure occurs, thereby defining the inert, residual-stress-sensitive strength $\sigma_a = \sigma_m = \sigma_i$. The idealized Griffith crack follows as the limiting case $\chi_r = 0$ in Equation 1, whence failure occurs spontaneously at the initial crack size $c = c_0'$, defining the inert, residual-stress-free strength $\sigma_a = \sigma_i^0 = K_c/(\pi\Omega c_0')^{1/2}$. It is noted that $c_0'$ does not appear in Equation 3, i.e. the inert strength does not depend on the initial conditions, provided $c_0' < c_m$.

Turning now to dynamic fatigue, we allow that crack growth can proceed along a subcritical path $K < K_c$ according to some rate-dependent condition. This condition is generally expressed in terms of a crack velocity function, $v(K)$, most simply in power-law form

$$v = v_0\left(\frac{K}{K_c}\right)^n \qquad (K < K_c), \quad (4)$$

where $v_0$ and $n$ are constants to be determined empirically for any given material/environment system. At $K > K_c$ the crack expands relatively rapidly, limited only by the inertia of the system. Generally, the $v(K)$ curve in the subcritical domain has more than one branch, corresponding to different mechanisms of rate control [1]. Three regions are commonly distinguished: (i) Region I, at low $K$, with velocity controlled by rate of reaction between environmental species and crack-tip bonds (with the possibility of a zero-velocity threshold in $K$, corresponding to a fatigue limit in the strength); (ii) Region II, at intermediate $K$, a transport-controlled region where the velocity curve tends to a plateau; (iii) Region III, at high $K$, a steeply rising section of the curve, independent of the environment. Of these three regions it is Region I which is usually the most important, since the crack kinetics are determined predominantly by the stages of slowest growth. Thus, writing $\sigma_a = \dot{\sigma}_a t$, with the stress rate $\dot{\sigma}_a$ constant in dynamic fatigue,

we may combine Equations 1 and 4 to obtain the following differential equation for crack size in terms of time

$$\frac{\dot{c}}{v_0} = \left\{ \left[ \frac{\chi_r}{K_c} \right] \frac{P}{c^{3/2}} + \left[ \frac{(\pi\Omega)^{1/2}}{K_c} \right] \dot{\sigma}_a c^{1/2} t \right\}^n . \quad (5)$$

This differential equation must be solved by an integration procedure for the time to failure $t_f$, adjusting the parameters $v_0$ and $n$ where necessary to accommodate a multi-region crack velocity function, the final critical crack size being determined by the instability requirement $K = K_c$, $dK/dc > 0$ in Equation 1. With $t_f$ thus determined the strength $\sigma = \dot{\sigma}_a t_f$ follows, so allowing for construction of a dynamic fatigue function $\sigma(\dot{\sigma}_a)$.

In general, the integration of Equation 5 has to be carried out numerically. An important exception is in the Griffith limit $\chi_r = 0$, with a single-region (Region I) crack velocity function, whence the standard analytical solution

$$\sigma^0 = (\lambda \dot{\sigma}_a)^{1/(n+1)} \qquad (\sigma^0 < \sigma_i^0) \quad (6)$$

is obtained, where

$$\lambda = \left[ \frac{2(n+1)}{(n-2)} \right] \left[ \frac{K_c}{(\pi\Omega)^{1/2}} \right]^n \Big/ v_0 c_0'^{\,n/2-1} .$$

Thus the slope and intercept of the dynamic fatigue curve in logarithmic co-ordinates contains information which allows, in principle, for a determination of the basic parameters $v_0$ and $n$. One of our aims is to devise a scheme for obtaining similar information from the fatigue curve for as-indented test pieces.

## 2.2. Analysis of fatigue equation using reduced variables

Equation 5 contains numerous variables, representing the loading conditions $(P, \dot{\sigma}_a)$, configurational constants $(\chi_r, \Omega)$ and material $(K_c)$ and material/environment $(v_0, n)$ fracture parameters. At this stage it is convenient to adopt a normalization procedure, and so avoid as far as possible having to specify these quantities. We accordingly follow our previous course [5, 6], with one significant modification: instead of normalizing with respect to the crack configuration which defines the inert strength at *zero* residual contact stress $(\sigma_i^0, c_0')$, we now choose the corresponding configuration at *non-zero* residual stress $(\sigma_m, c_m)$ as our reference state. Not only is this modification appropriate in terms of our stated aim of taking fatigue data exclusively from as-indented test pieces (Section 1), it also usefully eliminates one degree of freedom in the fatigue analysis, as we shall demonstrate below.

Reduced variables are thus introduced as follows:

$$\mathscr{S}_a = \sigma_a/\sigma_m \quad (7a)$$

$$\mathscr{C} = c/c_m \quad (7b)$$

$$\mathscr{T} = tv_0/c_m \quad (7c)$$

$$\mathscr{K} = K/K_c . \quad (7d)$$

Then Equation 1 simplifies to

$$\mathscr{K} = \frac{1}{4\mathscr{C}^{3/2}} + \frac{3\mathscr{S}_a\mathscr{C}^{1/2}}{4} . \quad (8)$$

The function $\mathscr{K}(\mathscr{C})$ is plotted in Fig. 2, for several values of $\mathscr{S}_a$. Two equilibrium crack dimensions $(\mathscr{K} = 1)$ of special interest are indicated: $\mathscr{C}_0 = 0.397$, corresponding to the initial, stable configuration at $\mathscr{S}_a = 0$; $\mathscr{C}_m = 1$, corresponding to the critical, unstable configuration at $\mathscr{S}_a = \mathscr{S}_m = 1$, which determines the inert strength $\mathscr{S}_i$ for as-indented test pieces. For tests in a reactive environment at constant stress rate $\dot{\mathscr{S}}_a = \mathscr{S}_a/\mathscr{T}$ the crack grows from its initial size along some subcritical path $\mathscr{K} < 1$ until the instability condition $\mathscr{K} = 1$, $d\mathscr{K}/d\mathscr{C} > 0$ is attained, the final crack configuration $\mathscr{C} = \mathscr{C}_f > 1$ at this point determining the dynamic fatigue strength $\mathscr{S}_a = \mathscr{S} < 1$.

Formal analysis of the fatigue characacteristics proceeds by rewriting the crack velocity function in Equation 4 in reduced form, $\dot{\mathscr{C}} = d\mathscr{C}/d\mathscr{T} = \mathscr{K}^n$, whence we obtain, in analogy to Equation 5,

$$\dot{\mathscr{C}} = \left( \frac{1}{4\mathscr{C}^{3/2}} + \frac{3\dot{\mathscr{S}}_a\mathscr{C}^{1/2}\mathscr{T}}{4} \right)^n . \quad (9)$$

Thus, once the stress rate is specified we have only one adjustable, the kinetic parameter $n$. With our previous normalization scheme [5, 6] a second adjustable, relating to the residual-stress term $\chi_r$, appeared in the formulation; in the present case this term has been incorporated into the reference crack dimension $c_m$, Equation 3b. Solutions of the differential equation in Equation 9 for the reduced time to failure $\mathscr{T}_f$ may now be obtained by numerical integration. At this point an important simplification concerning the initial conditions may be introduced into the analysis. In our earlier

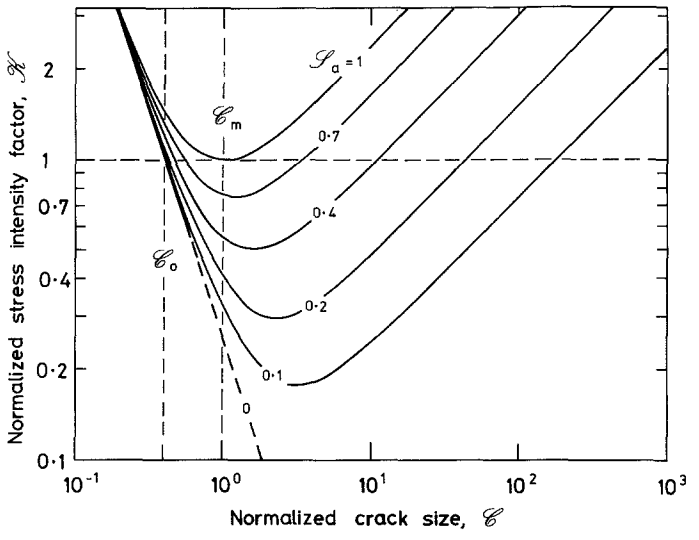


*Figure 2* Normalized plot showing stress intensity factor for indentation flaw as a function of characteristic dimension, at several levels of applied stress.

fatigue study of indentation flaws in glass [6] it was shown that the time to failure was insensitive to whether $c_0$ or $c_0'$ was taken as the starting dimension (with $c_0'$ typically $\approx 50\%$ in excess of $c_0$). The explanation for this behaviour lies in the fact that the function $\mathscr{K}(\mathscr{C})$ in Fig. 2 has a minimum between $\mathscr{C}_0$ and $\mathscr{C}_f$; the crack velocity is therefore lowest in the intermediate region, which accordingly controls the kinetics. We thus appear to be justified in taking $\mathscr{T} = 0$, $\mathscr{C} = \mathscr{C}_0 = 0.397$ as an invariant initial condition, rather than having to specify $\mathscr{C}_0'$ as a further adjustable. A proviso for this step to remain a good approximation is that the condition $\mathscr{C}_0' < 1$ be satisfied, corresponding to $c_0' < c_m$ in absolute terms; we recall from Section 2.1 that this is the same condition that needs to be satisfied in order that the inert strength be independent of starting flaw size.

Fig. 3 shows the results of numerical solutions of Equation 5, using a Runge–Kutta procedure,* plotted logarithmically in the standard form $\mathscr{S}(\dot{\mathscr{S}}_a)$ for selected values of $n$ appropriate to a single-region crack velocity function. It is noted that each curve becomes closely linear in the fatigue region $\mathscr{S} < \mathscr{S}_i$ (the more so at higher $n$) in which case we may write, in direct analogy to Equation 6,

$$\mathscr{S} = (\Lambda' \dot{\mathscr{S}}_a)^{1/(n'+1)} \quad (\mathscr{S} < \mathscr{S}_i), \qquad (10)$$

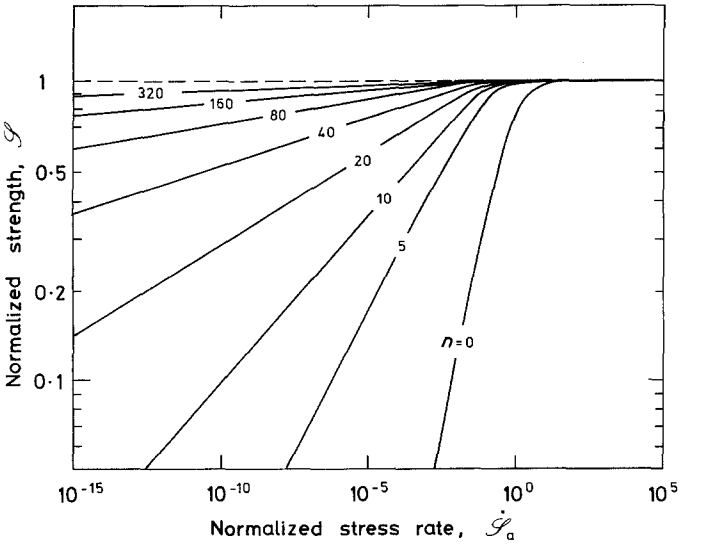


*Figure 3* Normalized dynamic fatigue curves for as-indented specimens, computed for selected values of $n$.

*See any standard text on numerical methods.

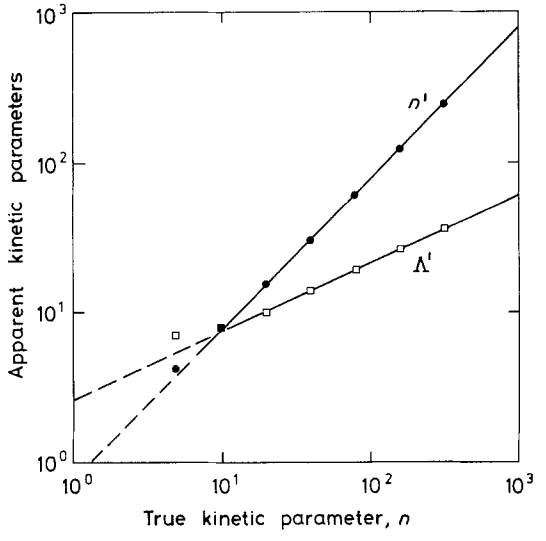


*Figure 4* Plot showing variation of $n'$ and $\Lambda'$ as a function of $n$. Points are from slope/intercept evaluations of curves in Fig. 3 in accordance with Equation 10.

where the primes are used here to indicate that the adjustables relate to residual-stress-sensitive conditions. The variation of these adjustables, from slope and intercept determinations over the stress-rate range $10^{-10} < \dot{\mathscr{S}}_a < 10^{-2}$, is shown in Fig. 4 as a function of $n$. Again, the logarithmic co-ordinates allow for linear fits, giving empirical relations

$$n' = 0.763n \tag{11a}$$

and

$$\Lambda' = 2.51n^{0.462} \tag{11b}$$

which are accurate to $\approx 1\%$ for $n$ and $\approx 10\%$ for $\Lambda'$ in the region $n > 10$ (the accuracy declining markedly for smaller values of $n$).

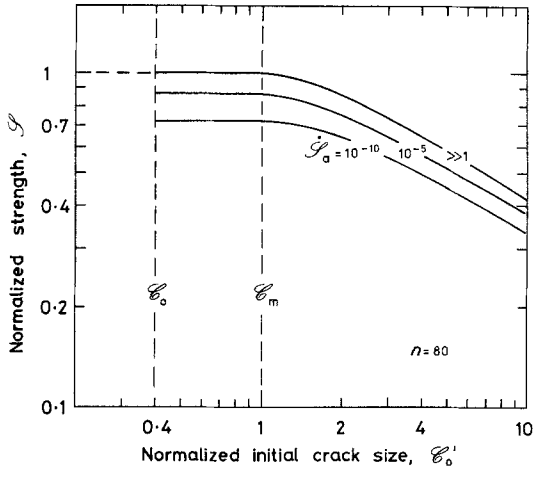


*Figure 5* Normalized plot illustrating the effect of initial crack size on dynamic fatigue strength, at several levels of applied stress rate.

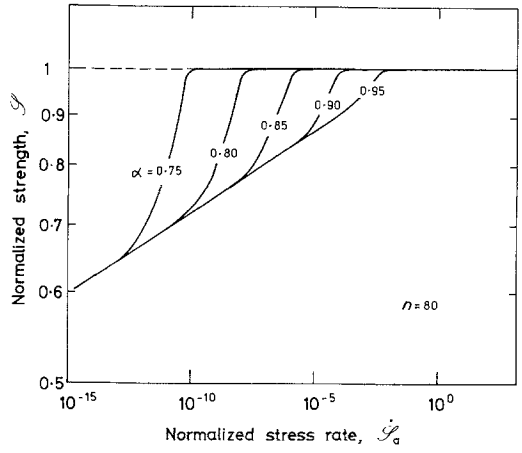


*Figure 6* Normalized plot illustrating effect of incorporating Region II crack velocity behaviour into dynamic fatigue analysis, for several values of truncation parameter $\alpha$.

Finally in this section, let us examine more closely the extent to which we are justified in making some of the assumptions which underlie the analysis.

### 2.2.1. Invariant initial condition

Accordingly, Fig. 5 shows, for $n = 80$, the effect on strength $\mathscr{S}$ of a variable initial crack size $\mathscr{C}_0'$. As anticipated, the results are insensitive to $\mathscr{C}_0'$ in the region $\mathscr{C}_0' < 1$. Beyond this region the fatigue strength function $\mathscr{S}(\dot{\mathscr{S}}_a)$ begins to diminish (corresponding to a depression of the curves in Fig. 3), and Equation 11 accordingly loses its accuracy.

### 2.2.2. Single-region crack velocity function

We may illustrate the point by incorporating a Region II plateau into the analysis. This is done by truncating the velocity at $\dot{\mathscr{C}} = \mathscr{V}_\alpha = \alpha^n$, $(0 < \alpha < 1)$, where $\alpha = K_\alpha/K_c$ defines a transition stress intensity factor. Recomputed fatigue curves for $n = 80$ are shown in Fig. 6. The influence of Region II clearly increases as $\alpha$ diminishes. Further modifications along these lines could be made to the computation to account for Region III behaviour where considered necessary.

### 2.2.3. Zero pre-indentation surface stress

In many cases a specimen, by virtue of its mechanical, thermal or chemical history, may exist in a state of significant surface pre-compression (or, in unfavourable instances, in pre-tension). The requi-

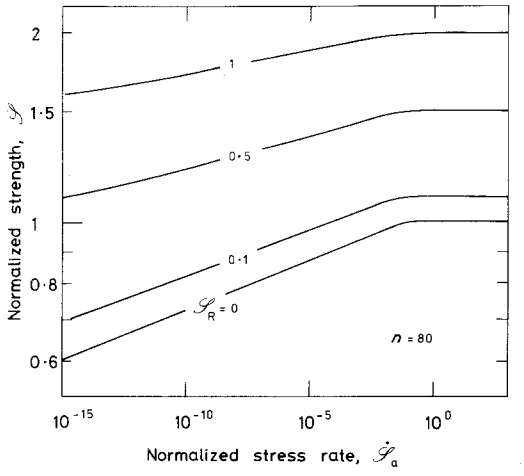


*Figure 7* Normalized plot illustrating effect of incorporating residual pre-indentation surface compression into dynamic fatigue analysis, for several values of $\mathscr{S}_R$.

site amendment to the analysis is straightforward, with $\sigma_a$ in Equation 1 replaced by $\sigma_a - \sigma_R$, where $\sigma_R$ is the residual compressive component (taken to be uniform over the crack area) [4]: equivalently, $\mathscr{S}_a$ in Equation 8 is replaced by $\mathscr{S}_a - \mathscr{S}_R$, with $\mathscr{S}_R = \sigma_R/\sigma_m$ ($\sigma_m$ still referring to inert strength at zero level of pre-compression). Carrying this substitution through the formulation to Equation 9, one may generate modified fatigue curves, as shown in Fig. 7 at $n = 80$ for selected values of $\mathscr{S}_R$.* It is evident that moderate levels of pre-existing surface stress can have a strong effect on the strength characteristics.

## 3. Discussion

We are now in a position to consider how we might obtain basic fracture parameters from dynamic fatigue data on as-indented specimens. The kinetic parameters are evaluated from the denormalized form of Equation 10, using Equation 7 to convert back to absolute quantities

$$\sigma = (\lambda' \dot{\sigma}_a)^{1/(n'+1)} \qquad (\sigma < \sigma_i), \quad (12)$$

where

$$\lambda' = \frac{\Lambda' \sigma_m^{n'} c_m}{v_0}. \quad (13)$$

In combination with Equation 11 we then obtain

$$n = 1.31n' \quad (14a)$$

and

$$v_0 = \frac{2.84n'^{0.462} \sigma_m^{n'} c_m}{\lambda'}. \quad (14b)$$

Hence the slope of the log $\sigma$ against log $\dot{\sigma}_a$ plot in the reaction-controlled region (low $\dot{\sigma}_a$) immediately determines $n$, via Equation 14a. For instance, in our earlier dynamic fatigue study of soda-lime glass in water [5] an "apparent" exponent $n' = 13.7 \pm 0.2$ was measured from data on as-indented specimens; the "true" exponent $n = 18.0 \pm 0.3$ duly computed from Equation 14a compares favourably with the value $n = 17.9 \pm 0.5$ measured in the same earlier study from comparative data on specimens subjected to a post-indentation anneal (i.e. specimens of zero residual stress, for which Equation 6 replaces Equation 12). The parameter $v_0$ similarly follows from the intercepts of the fatigue plot; in this case, however, a complete determination from Equation 14b cannot be made without knowledge of $\sigma_m$ and $c_m$. Experimentally, $\sigma_m$ is measured readily as the inert strength $\sigma_i$, but $c_m$ requires additional, direct observation of the critical crack configuration (see Part 2). Once $\sigma_m$ and $c_m$ are known, Equation 3 provides an estimate of the terms $K_c/(\pi\Omega)^{1/2}$ and $K_c/\chi_r$. Absolute solutions of Equation 5 may now be obtained for any given loading conditions, thereby allowing for an evaluation of the crack evolution from the true initial size $c_0'$ to failure.

Although we have focussed our attention on dynamic fatigue, the theory outlined in Section 2 is not restrictive. Thus to derive solutions for static fatigue it is necessary only to replace $\dot{\sigma}_a t$ in Equation 5 by a constant $\sigma_a$, and to integrate as before. A demonstration of the procedure is given by Chantikul *et al.* [6], where parameters calibrated from dynamic fatigue data are used to predict static fatigue lifetimes for the glass–water system.

The above analysis also establishes a basis for deriving the crack velocity curve. Of course, the form of the $v(K)$ function must be specified beforehand; in the present scheme the process of

*In fact, the curves in Fig. 7 may be generated, to excellent approximation, simply by adding $\mathscr{S}_R$ to the appropriate $\mathscr{S}(\mathscr{S}_a)$ curve in Fig. 3. The reason for this is as follows. Suppose that we apply the stress $\mathscr{S}_a$ until the surface compression $\mathscr{S}_R$ is exactly negated. Under *inert* conditions the crack would then attain the equilibrium length $\mathscr{C}_0$ [4], which corresponds to the initial condition for unstressed surfaces. Hence the strength value is augmented in a direct manner by the pre-existing surface stress. Under *non-inert* conditions the crack at the stress-negation configuration may extend subcritically beyond $\mathscr{C}_0$. However, we have already seen, via Fig. 5, that the fatigue strength is reasonably independent of the initial condition. Hence the simple additivity operation remains effectively valid under all conditions.

fitting data on a fatigue plot does no more than provide values for the adjustable kinetic parameters. With $n$ and $v_0$ thus determined in Equation 4, it remains only to specify $K_c$. (For materials of unknown toughness, an estimate can be conveniently obtained from the quantity $\sigma_m P^{1/3}$ in the inert-strength region, using data from selected reference materials to calibrate Equation 3 in an appropriate manner [15].) For cases in which a multi-region $v(K)$ function is evident, a linear fitting procedure is practicable only with Region I: with Regions II and III a trial-and-error approach is probably the simplest means of parameter adjustment, e.g. by interpolation from plots of the type shown in Fig. 6.

We have stipulated the condition $c_0' < c_m$ as a proviso for the validity of the integration procedure adopted in Section 2.2. Violation of this condition might occur via either of the following post-indentation processes: (i) excessive increase in $c_0'$, due to subcritical crack growth in a reactive environment; (ii) excessive decrease in $c_m$ (see Equation 3b), due to residual-stress relief (e.g. by lateral crack development, surface grinding or annealing). Fortunately, such violation is expected to be the exception rather than the rule with Vickers indentations on most brittle materials [7, 15]. (If $c_0'$ *were* to exceed $c_m$, then Equations 3 and 14 would, at best, allow for first-approximation estimates of adjustable parameters, in which case the fitting of Equation 5 to the data might require an iteration procedure.) There is an implied tendency here for some of the non-kinetic parameters to be subject to a certain degree of variability during the total crack evolution to failure. It is for this reason that it is considered preferable to determine the normalization quantities $\sigma_m$ and $c_m$ by direct experimental observation under the actual conditions of testing, rather than through efforts to predetermine $\Omega$ and $\chi_r$ (either by first-principles calculation or by calibration from data on "model" materials) in Equation 3.

It is important to emphasize that the present analysis relates entirely to fatigue characteristics of test specimens in the *as-indented* state. By incorporating a residual contact term into the stress intensity factor for the indentation flaws we avoid all the potential complications which would inevitably attend any attempt to remove the associated residual stresses by physical means. Data may be processed in much the same way as in current conventional dynamic fatigue analysis [16]; it needs only to be recognised that the kinetic parameters so determined are apparent rather than true values, and that appropriate conversion formulae such as those in Equation 14 must be invoked. This approach makes for extreme simplicity in the experimental test programme, with the usual benefits of relatively high reproducibility in results, specimen economy, etc. which characterize indentation fracture techniques [12]. Of course, this does not eliminate the ultimate need to obtain information on the flaw populations of prospective in-service components. Our method simply enables us to treat the materials evaluation aspect of strength analysis in isolation from flaw statistics.

While it should be unnecessary to remove any residual stresses from the specimen surface after indentation, the same may not be true of the specimen state before indentation. We indicated briefly in Section 2.2 that surface preparation can lead to significant levels of pre-compression (or pre-tension). Indeed, the deliberate introduction of surface compressive stresses can be a most effective means of strengthening brittle materials. However, for the immediate purpose of parameter evaluation the presence of such stresses serves only to complicate the analysis, not least by causing deviations from linearity in the fatigue plots (Fig. 7) and is accordingly best avoided where possible (unless, of course, the surface compression is itself part of the evaluation).

In conclusion, we should acknowledge that the use of controlled flaws for producing "universal" fatigue curves is by no means new. The concept derives from the early work of Mould and Southwick [17], who studied the fatigue properties of abraded glass surfaces. Although widely adopted by many subsequent workers in strength-testing programmes, abrasion flaws are comparatively ill-defined entities, in addition to which it is not usually possible to identify the prospective failure site prior to testing. Consequently, specification of quantities such as $P$, $c_0'$ and $c_m$ is not straightforward as it is for indentation flaws. Furthermore, because of an increased tendency for abrasion flaws to chipping, especially in the regions of overlap with neighbouring damage sites, relief of residual stress is accentuated; in the case of glass this is sufficient to make $c_m < c_0'$ [18]. With natural flaws the quantity $\chi_r$ appropriate to Equation 5 will be very much a function of specimen history; in this context the indentation studies provide valuable

insight into the departures that might be expected from idealized Griffith behaviour.

## Acknowledgements

The authors wish to thank P. Kelly for assistance with the computations. Funding for this work was provided by the Australian Research Grants Committee.

## References

1. S. M. WIEDERHORN, "Fracture Mechanics of Ceramics", Vol. 2, edited by R. C. Bradt, D. P. H. Hasselman and F. F. Lange (Plenum, New York, 1974) p. 613.
2. B. R. LAWN and D. B. MARSHALL, "Fracture Mechanics of Ceramics", Vol. 3, edited by R. C. Bradt, D. P. H. Hasselman and F. F. Lange (Plenum, New York, 1978) p. 205.
3. D. B. MARSHALL and B. R. LAWN, *J. Mater. Sci.* **14** (1979) 2001.
4. D. B. MARSHALL, B. R. LAWN and P. CHANTIKUL, *ibid.* **14** (1979) 2225.
5. *Idem*, *J. Amer. Ceram. Soc.* **63** (1980) 532.
6. P. CHANTIKUL, B. R. LAWN and D. B. MARSHALL, *ibid.* **64** (1981), to be published.
7. B. R. LAWN, A. G. EVANS and D. B. MARSHALL, *ibid.* **63** (1980) 574.
8. B. R. LAWN and T. R. WILSHAW, "Fracture of Brittle Solids" (Cambridge University Press, London, 1975) Ch. 2.
9. J. J. PETROVIC, R. A. DIRKS, L. A. JACOBSON and M. G. MENDIRATTA, *J. Amer. Ceram. Soc.* **59** (1976) 177.
10. J. J. PETROVIC and M. G. MENDIRATTA, "Fracture Mechanics Applied to Brittle Materials", edited by S. W. Freiman (ASTM Special Technical Publication 678, Philadelphia, 1979) p. 83.
11. B. R. LAWN and M. V. SWAIN, *J. Mater. Sci.* **10** (1975) 113.
12. B. R. LAWN and T. R. WILSHAW, *ibid.* **10** (1975) 1049.
13. B. R. LAWN and E. R. FULLER, *ibid.* **10** (1975) 2016.
14. B. R. LAWN, D. B. MARSHALL and P. CHANTIKUL, *ibid.* **16** (1981) 1769.
15. P. CHANTIKUL, G. R. ANSTIS, B. R. LAWN and D. B. MARSHALL, *J. Amer. Ceram. Soc.* **64** (1981), to be published.
16. S. M. WIEDERHORN and J. E. RITTER, "Fracture Mechanics Applied to Brittle Materials", edited by S. W. Freiman (ASTM Special Technical Publication 678, Philadelphia, 1979) p. 202.
17. R. E. MOULD and R. D. SOUTHWICK, *J. Amer. Ceram. Soc.* **42** (1959) 542, 582.
18. D. B. MARSHALL and B. R. LAWN, *Comm. Amer. Ceram. Soc.* **64** (1981) C6.

Received 17 February and accepted 26 March 1981.